Single-Photon Source Based on FWM With Adjustable Linear SOP

Álvaro J. Almeida, Nuno A. Silva, Nelson J. Muga[1], and Armando N. Pinto

[1] Departamento de Física, Universidade de Aveiro, 3810-193 Aveiro, Portugal

***Abstract* – We present a setup able to generate and detect single photons in optical fibers using the stimulated four-wave mixing (FWM) process. The results show an accurate generation of single photons at four different linear states of polarization (SOPs), with angles 0, 45, 90 and -45 degrees. The detection was performed in back-to-back configuration and after transmission over an optical fiber with a length up to 10 m.**

***Keywords* – Single-Photon Source, Polarization Control, Four-Wave Mixing, State of Polarization.**

I. INTRODUCTION

The security of public-key cryptographic systems could become vulnerable due to advances in mathematics or computation [1]. Moreover, quantum cryptography offers us a practical solution to transmit secure information between two identities, usually called Alice and Bob [2]. The security of the transmitted information is assured by quantum mechanics properties such as no-cloning theorem and the Heisenberg uncertainty principle [3]. This means that quantum cryptography is not vulnerable to theoretical or technological advances [1]. The main application of quantum cryptography is the Quantum Key Distribution (QKD). In terms of encoding methods, QKD can be implemented using polarization- or phase-encoding [3].

Stephen Wiesner first proposed quantum cryptography in 1970, although more than 10 years have passed before his paper was finally published [4]. Using Wiesner's work, in 1984, Bennett and Brassard created the first quantum protocol, the well known BB84 [5]. The first QKD experiment using polarization-encoding for the BB84 protocol took place in 1989 and was performed in free-space over 32.5 cm [6], [7]. Besides BB84 many other quantum protocols were designed. One of them is the 2-state protocol, also known as B92 that needs only two non-orthogonal states to implement secure QKD [8]. A more secure, but also more difficult to implement, quantum protocol, is the 6-state protocol, that uses three non-orthogonal bases that Alice and Bob randomly alternate [9], [10]. A very suitable QKD protocol called Differential-Phase-Shift Quantum Key Distribution (DPS-QKD) is now emerging as a technology that can be deployed in real fiber optical networks, and it is inherently secure against strong eavesdropping attacks called Photon Number-Splitting (PNS) attacks [1], [11].

Most of the quantum protocols require single-photon sources in order to transmit information between two different locations [12]. Single-photon sources can be obtained from many devices, such as color centers in diamond, quantum dots, or single atoms and molecules [13]. However, these sources have some practical problems, such as low collection efficiency, the technological complexity or the stability of the molecules [13]. Recently, stimulated FWM has been used to generate single-photons in optical fibers [14]-[18]. The stimulated FWM process is a third-order nonlinear process that occurs when light of two or more frequencies (known as pump and signal fields) are launched into an optical fiber given rise to a new wave, known as idler field [19]. One advantage of using the stimulated FWM is the possibility of generating the photons already inside the optical fiber [14], [15], [17]-[19]. Polarization encoded photons have been proposed in some quantum experiments to implement quantum cryptography protocols in optical fibers [12].

In this paper, we use the stimulated FWM process to obtain a source of single photons with adjustable linear SOP. This source also has the advantage of using only one optical field to obtain four different linear SOPs.

This paper is organized in the following way: in section II we describe the experimental setup used to generate and detect single photons in four different linear SOPs. In section III we present a theoretical description of the experiment. In section IV the experimental results are presented and discussed. Finally, in section V we present our conclusions.

II. EXPERIMENTAL DESCRIPTION OF THE SINGLE-PHOTON SOURCE

In the experimental setup, see Fig. 1, a pump at λ_1 from a external cavity laser (ECL), passes through a polarization controller (PC1), before being coupled to another optical signal, λ_2, from a tunable laser source (TLS). This second optical signal, λ_2, is externally modulated to produce optical pulses with a width at half maximum of 1.6 ns and a repetition rate of 555.6 kHz. The two optical fields, λ_1 and λ_2, pass through a linear polarizer, P1, and are launched into a dispersion-shifted fiber (DSF), with a length equal to 305 m. Due to the stimulated FWM process, a new optical field, called idler, is generated inside the DSF at $\lambda_3 = \lambda_1\lambda_2/(2\lambda_2 - \lambda_1)$ [19]. At the fiber output, the three optical fields pass through the PC4 in order to align the SOP of the idler photons with the linear polarizer P2. A filter, F1, blocks the pump and signal waves. At the exit of P2 the angle of the linear SOP, θ_1, is controlled using a

rotatable key connector (RKC1). After passing through the quantum channel (optical fiber), the SOP of the idler photons is analyzed using another linear polarizer, P3, whose orientation, θ_2, is tuned using a second RKC (RKC2). The idler photons from P3 are detected with a Single-Photon Detector Module (SPDM) operating in the Geiger mode. The dark count probability of the SPDM for a time gate, t_g = 2.5 ns, is $P_{dc} = 5\times10^{-5}$, and the quantum detection efficiency is η = 10 % [20]. Photon counting measurements were performed with 0.1 photons per pulse at the input of the quantum channel, during a period of time of 10 s.

III. THEORETICAL DESCRIPTION

In order to asses if the SOPs are correctly generated and detected, we present here a theoretical description that allows to evaluate the obtained experimental data.

From the definition of Stokes polarization parameters (S_0, S_1, S_2 and S_3) for a plane wave, we can write the total optical power as,

$$S_0 = \sqrt{S_1^2 + S_2^2 + S_3^2}. \quad (1)$$

The parameter S_1 is the difference between the optical power that passes through a linear horizontal polarizer and a linear vertical polarizer. The parameter S_2 is the difference between the optical power that passes through a linear polarizer at +45° and a linear polarizer at -45°, and S_3 is the difference between the optical power that passes through a circular right polarizer and circular left polarizer [21].

The SOP at P3 output (see Fig. 1) can be written as,

$$S'(2\theta) = M_P(2\theta) S_i, \quad (2)$$

where $M_P(2\theta)$ is the Mueller matrix for a rotated linear polarizer in Stokes space, and S_i is the Stokes vector corresponding to the SOP at the fiber link output. The Mueller matrix for a rotated ideal linear polarizer is given by [21],

$$M_P(2\theta) = \frac{1}{2}\begin{bmatrix} 1 & \cos(2\theta) & \sin(2\theta) & 0 \\ \cos(2\theta) & \cos^2(2\theta) & \sin(2\theta)\cos(2\theta) & 0 \\ \sin(2\theta) & \sin(2\theta)\cos(2\theta) & \sin^2(2\theta) & 0 \\ 0 & 0 & 0 & 0 \end{bmatrix}, \quad (3)$$

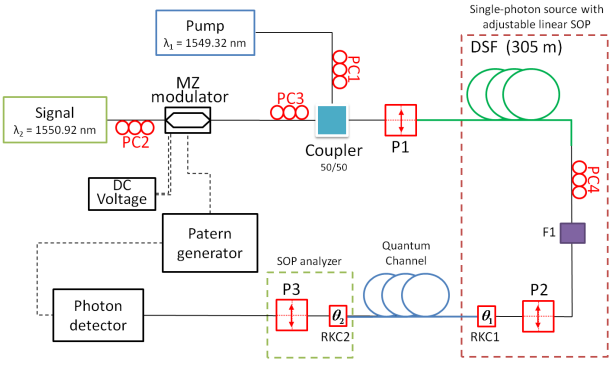

Figure 1 - Experimental setup used to generate and detect single photons at the linear SOPs with angles 0, 45, 90 and -45 degrees. Details of the setup are presented in the text.

where θ is the angle of the analyzer, see Fig. 1, which can vary between 0 and π. The Stokes vector corresponding to the SOP at the fiber link output can be written as [21],

$$S_i(2\alpha, 2\beta) = \begin{bmatrix} S_0 \\ S_1 \\ S_2 \\ S_3 \end{bmatrix} = S_0 \begin{bmatrix} 1 \\ \cos(2\alpha)\cos(2\beta) \\ \cos(2\alpha)\sin(2\beta) \\ \sin(2\alpha) \end{bmatrix}, \quad (4)$$

where α represents the ellipticity of the SOP, that can vary between $-45°$ and 45°, and β is the orientation of the semi-major axis of the ellipse, which can vary between 0° and 180°. Note that α and β angles are refereed to the Stokes space. Substituting (3) and (4) in (2), we obtain,

$$S'(2\theta, 2\alpha, 2\beta) = \frac{S_0}{2}\begin{bmatrix} 1+\cos(2\alpha)\cos(2(\beta-\theta)) \\ \cos(2\theta)[1+\cos(2\alpha)\cos(2(\beta-\theta))] \\ \sin(2\theta)[1+\cos(2\alpha)\cos(2(\beta-\theta))] \\ 0 \end{bmatrix}. \quad (5)$$

From (5), we can obtain the four Stokes polarization parameters. Using (1), we can write the total optical power at P3 output, as,

$$S'_0(2\theta, 2\alpha, 2\beta) = \frac{S_0}{2}\left[1+\cos(2\alpha)\cos(2(\beta-\theta))\right]. \quad (6)$$

In terms of the average number of counts, (6) can be written as,

$$\mathcal{F}(2\theta, 2\alpha, 2\beta) = \frac{\overline{N}}{2}\left[1+\cos(2\alpha)\cos(2(\beta-\theta_2))\right], \quad (7)$$

where $\mathcal{F}$ is the average number of counts for each SOP, and $\overline{N}$ represents the average number of counts for a linear SOP, i.e., $\alpha = 0°$, aligned with the polarizer angle, i.e., $\beta = \theta_2$.

IV. ANALYSIS OF THE EXPERIMENTAL RESULTS

In this section we present and discuss the experimental results obtained for the three different schemes: (i) back-to-back configuration, and (ii) 1 m of transmission fiber and (iii) 10 m of transmission fiber.

A. Back-to-Back

First, we performed a measurement without the quantum channel, where the RKC1 was in back-to-back with the RKC2, i.e., the two RKCs was directly linked.

In Fig. 2 we plot the average number of counts as a function of θ_2, for the four different linear SOPs generated by our single-photon source. The results presented in Fig. 2 show that it exists a maximum and a minimum, separated of about 90°, for each linear SOP. The mean phase difference between each linear SOP is about 45°. The fact that the maximums do not present the exact same value is because the losses are different for different angles of the RKCs.

The theoretical fits given by (7) are also plotted in Fig. 2. We can see a good adjustment to the experimental results, which means that the experimental data for this scheme

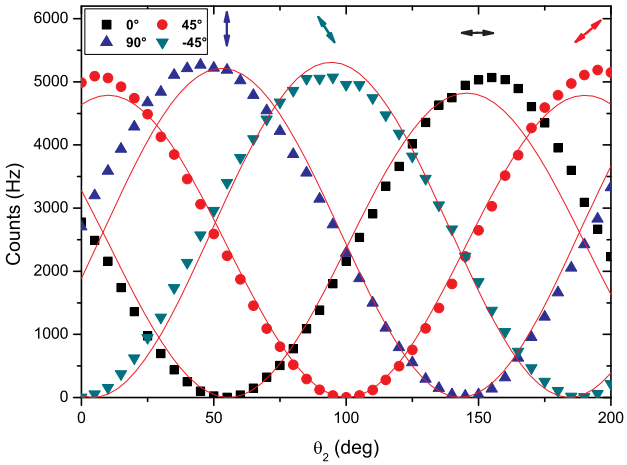

Figure 2 - Average number of counts (Hz) as a function of the angle θ_2 (degrees), for the linear SOPs with angles $\theta_1 = 0$, 45, 90 and -45 degrees, for back-to-back. θ_1 is the angle of the single-photon source, and θ_2 is the angle of the analyzer. The pump and signal optical powers at the fiber input were P_1 = 2.20 mW, and P_2 = 0.69 mW, respectively. The wavelengths for the pump and the signal were λ_1 = 1549.32 nm and λ_2 = 1550.92 nm, respectively. The theoretical fits given by (7) are represented by the solid lines.

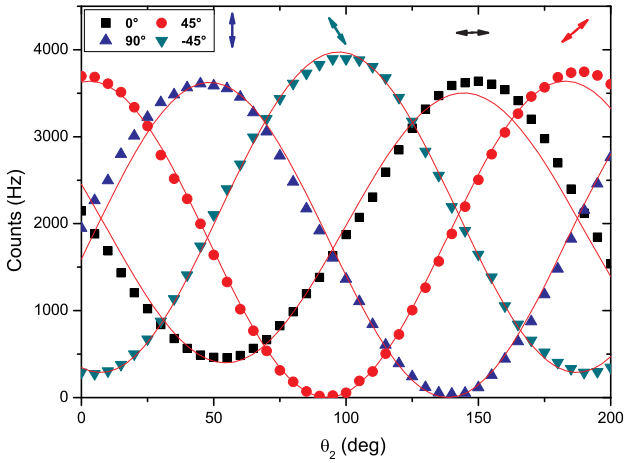

Figure 3 - Average number of counts (Hz) as a function of the angle θ_2 (degrees), for the linear SOPs with angles $\theta_1 = 0$, 45, 90 and -45 degrees, using a SMF with a length equal to 1 m, as a quantum channel. θ_1 is the angle of the single-photon source, and θ_2 is the angle of the analyzer. The pump and signal optical powers at the fiber input were P_1 = 2.07 mW, and P_2 = 0.61 mW, respectively. The wavelengths are the same used in Fig. 2. The theoretical fits given by (7) are represented by the solid lines.

were well achieved. However, some minor deviations between theoretical and experimental results are observed. These are mainly due to the wear of the RKCs that are directly linked, and consequently lead to different losses for different angles of the RKCs.

From this analysis we can conclude that the generated single-photons were detected efficiently, and we can establish a good correspondence between the emitter and the receiver.

B. Propagation on a Single-Mode Fiber

In this subsection we report the obtained experimental data in the case where a SMF was used as a quantum channel. We have used two different fibers lengths, 1 and 10 m.

B.1 Length equal to 1 m

In Fig. 3 we present the average number of counts obtained with a SMF with a length equal to 1 m as a function of θ_2, for the four different linear SOPs. From Fig. 3, we also can see that exists a maximum and a minimum separated of about 90° for each linear SOP. In this scheme, the mean phase difference between the different linear SOPs, is about 48°. The minimum value obtained for 0 and -45 degrees present a slightly deviation from zero. This is due to a small polarization change inside the fiber that turns the SOP slightly elliptically polarized. A decrease of about 1500 counts in comparison with back-to-back is observed for this scheme. This is mainly due to insertion losses, since the fiber losses for this fiber length are negligible.

The theoretical fits presented in Fig. 3 have a good adjustment to the experimental data for the four different linear SOPs. The slightly deviations between the theoretical fit and the experimental results are mainly due to different losses for different angles of the RKCs.

B.2 Length equal to 10 m

In Fig. 4 we present the average number of counts obtained with a SMF with a length equal to 10 m as a function of θ_2, for the four different linear SOPs. The presence of a maximum and a minimum separated of about 90° for each SOP also maintains, as the decrease of about 1500 counts. The mean phase difference between the different linear SOPs is about 46°. However, between the SOPs of 0 and 45 degrees, that difference is about 60°. In terms of minimum values, we can see that only one SOP remains linear (45°), while the other three present some ellipticity due to polarization changes inside the optical fiber. The theoretical fits approximate well to the experimental data in the four different SOPs.

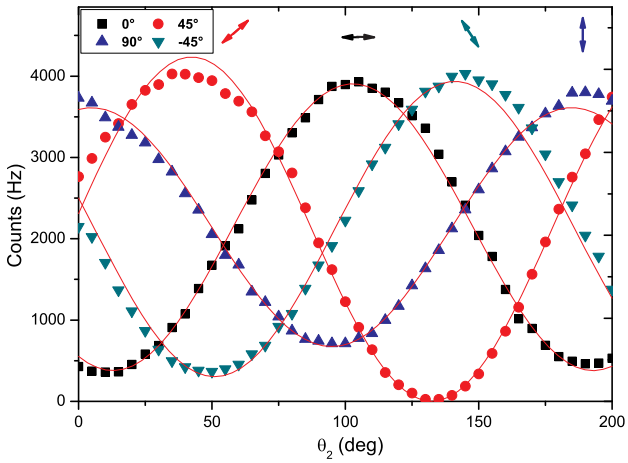

Figure 4 - Average number of counts (Hz) as a function of the angle θ_2 (degrees), for the linear SOPs with angles $\theta_1 = 0$, 45, 90 and -45 degrees, using a SMF with a length equal to 10 m, as a quantum channel. θ_1 is the angle of the single-photon source, and θ_2 is the angle of the analyzer. The optical powers and the wavelengths are the same used in Fig. 2. The theoretical fits given by (7) are represented by the solid lines.

For a SMF with a length longer than 10 m the results begins to deviate considerably from the theoretical description, since the polarization mode dispersion (PMD) assumes a major importance. PMD is a well known problem in optical communication systems [22]-[24]. This is due to the fact that birefringence varies randomly in an optical fiber, changing the SOP also randomly [25], [26]. This so-called modal birefringence, $B_m = |n_x - n_y|$, where n_x and n_y are the modal refractive indices for the two orthogonally polarized states, with $n_x \neq n_y$, randomly change the orientation of x and y axes over a length scale of $\sim$ 10 m, unless polarization-maintaining fibers (PMFs) were used [19]. This is the major issue of polarization-encoding in optical fibers. Due to this impairment we are unable to obtain a secure transmission in a fiber with a length longer than 10 m. To mitigate this impairment, some birefringence compensator will be needed, in order to control the SOP over the optical fiber [25], [26].

C. Visibility, Ellipticity and Orientation of the Ellipse

In order to perform a better evaluation of the experimental results, we can introduce a quantity that is called visibility. The visibility of the average number of counts, for each SOP, can be calculated as [27],

$$\mathcal{V} = \frac{M-m}{M+m}, \tag{8}$$

where M and m are, respectively, the maximum and minimum average number of counts for each SOP. Since the visibility can assume values between 0 and 1, the results for a linear SOP are considered ideal when it is equal to 1. The visibility values for each SOP, given by (8), are presented at Table I. In the table we also present the ellipticity and the orientation of the semi-major axis of the ellipse. These values were obtained from the theoretical fits to the experimental results.

Analyzing the Table I, we can conclude, from the visibility and ellipticity values, that for back-to-back case, all the SOPs presented at Fig. 2 have similar values for maximum and minimum average number of counts, and are all linearly polarized.

From the values obtained with the SMF with a length equal to 1 m we can see that the SOPs of 0 and -45 degrees are not perfectly linear but present some ellipticity different than 1. This is due to some random polarizations changes inside the optical fiber, as mentioned before.

From the values obtained with the SMF with a length equal to 10 m we can see that three of the SOPs present ellipticity values greater than 15. It traduces the fact that these SOPs are slightly elliptically polarized, mainly viewed for the SOP of 90°, as can be seen from the visibility values.

In respect to the orientation of the semi-major axis of the ellipse, β, we can see that the mean phase difference between the four SOPs of each scheme is about 45°. However, for the third scheme (SMF, L = 10 m) we have two SOPs separated of about 60°, namely the SOPs of 0 and 45 degrees. This is due to the fact that in a fiber with such a length, the correlation between the SOPs begins to lose. The fact that the values of β for the SMF with a length equal to 10 m are so different from the other two, it is because in this case the SOPs suffered a random translation.

Table I

VISIBILITY, GIVEN BY (8), ELLIPTICITY AND ORIENTATION OF THE SEMI-MAJOR AXIS OF THE ELLIPSE, OBTAINED FROM THE THEORETICAL FITS, OF EACH SOP, FOR BACK-TO-BACK AND USING A SMF WITH LENGTHS EQUAL TO 1 AND 10 M.

Analysis \ SOP	0°	45°	90°	-45°
Visibility, $\mathcal{V}$				
Back-to-Back	0.999	0.999	0.991	0.998
SMF, L = 1 m	0.776	0.987	0.976	0.869
SMF, L = 10 m	0.832	0.988	0.685	0.834
Ellipticity, α (deg)				
Back-to-Back	1	1	1	1
SMF, L = 1 m	18.7	1	1	15
SMF, L = 10 m	17.3	1	23.4	15.5
Orientation of the ellipse, β (deg)				
Back-to-Back	145.6	10.1	53	94.3
SMF, L = 1 m	144.5	2.9	48.5	97.2
SMF, L = 10 m	102.9	42.4	4.9	141

If we compare the three schemes tested in terms of the three parameters presented at Table I, we can see that there are a degradation in the results obtained with the increase of the length of the fiber. First, for the SMF with a length equal to 1 m we have two linearly polarized and two slightly elliptically polarized SOPs. For the SMF with a length equal to 10 m we have only one linearly polarized SOP, and three slightly elliptically polarized SOPs. Second, the maximum value of ellipticity obtained with the SMF with a length equal to 1 m is smaller than the one for the SMF with a length equal to 10 m.

These results are in good agreement with other experiments reported in the literature [19].

Based on the above discussion, we can say that we are able to implement a 4-states protocol with our single-photon source using a SMF with a length up to 10 m as a quantum channel.

V. CONCLUSIONS

We have shown that it is possible to generate and detect single photons in well defined four linear SOPs using a SMF with a length up to 10 m, as a quantum channel. This setup can be used to implement a quantum protocol to authenticate classical messages with enhanced security.

Our single-photon source permits to select four linear SOPs separated of 45°, and has the advantage of generate the photons already inside the optical fiber using only one optical field.

To extend the transmission length behind 10 m, active polarization-tracking devices must be used in order to surpass the PMD limitation.

ACKNOWLEDGEMENTS

This work was partially supported by the Fundação para a Ciência e a Tecnologia - FCT, through the Laboratório

Associado (IT/LA) program, project “QuantTel - Quantum Secure Telecommunications” and “QuantPrivTel - Quantum Private Telecommunications” project (PTDC/EEA-TEL/103402/2008), FEDER and PTDC programs.

REFERENCES

[1] H. Takesue, T. Honjo, K. Tamaki, and Y. Tokura, “Differential phase shift quantum key distribution”, *ITU-T Kaleidoscope*, May 2009.

[2] N. Gisin, G. Ribordy, W. Tittel, and H. Zbinden, “Quantum cryptography”, *Reviews of Modern Physics*, vol. 74, pp. 145–195, Jan. 2002.

[3] H.-K. Lo and Y. Zhao, “Quantum Cryptography”, *ArXiv e-prints*, Mar. 2008.

[4] Stephen Wiesner, “Conjugate coding”, *SIGACT News*, vol. 15, no. 1, pp. 78–88, 1983.

[5] C. H. Bennett and G. Brassad, “Quantum cryptography: Public-key distribution and coin tossing”, *Proceedings of IEEE International Conference on Computers, Systems and Signal Processing, Bangalore, India*, pp. 175 – 179, Dec. 1984.

[6] C. H. Bennett and G. Brassad, “The dawn of a new era for quantum cryptography: The experimental prototype is working!”, *Sigact News*, vol. 20, no. 4, 1989.

[7] C. H. Bennett, F. Bessette, G. Brassard, L. Salvail, , and J. Smolin, “Experimental quantum cryptography”, *Journal of Cryptology*, vol. 5, no. 1, 1992.

[8] C. H. Bennett, “Quantum cryptography using any two nonorthogonal states”, *Physical Review Letters*, vol. 68, pp. 3121–3124, May 1992.

[9] D. Bruß, “Optimal Eavesdropping in Quantum Cryptography with Six States”, *Physical Review Letters*, vol. 81, pp. 3018–3021, Oct. 1998.

[10] H. Bechmann-Pasquinucci and N. Gisin, “Incoherent and coherent eavesdropping in the six-state protocol of quantum cryptography”, *pra*, vol. 59, pp. 4238–4248, June 1999.

[11] K. Inoue, E. Waks, and Y. Yamamoto, “Differential Phase Shift Quantum Key Distribution”, *Physical Review Letters*, vol. 89, no. 3, pp. 037902, June 2002.

[12] Dirk Bouwmeester, Artur K. Ekert, and Anton Zeilinger, *The Physics of Quantum Information*, 2000.

[13] M. Dusek, N. Lutkenhaus, and M. Hendrych, “Quantum Cryptography”, *ArXiv Quantum Physics e-prints*, Jan. 2006.

[14] P. F. Antunes, A. N. Pinto, and P. S. André, “Single-Photon Source by Means of Four-Wave Mixing Inside a Dispersion-Shifted Optical Fiber”, *Frontiers in Optics, OSA Technical Digest (CD) Optical Society of America*, Oct. 10 2006.

[15] Álvaro J. Almeida, Gil G. Fernandes, and Armando N. Pinto, “Single-Photon Source With Adjustable Linear SOP”, *Proc VII Symposium On Enabling Optical Networks and Sensors, Nokia Siemens Networks, Amadora, Portugal*, June 26 2009.

[16] N. J. Muga, M. C. F. Fugihara, M. Ferreira, and Armando N. Pinto, “Non-Gaussian ASE Noise in Raman Amplification Systems”, *IEEE/OSA Journal of Lightwave Technology*, vol. 27, no. 16, Dec. 2009.

[17] Nuno A. Silva, Nelson J. Muga, and Armando N. Pinto, “Influence of the Stimulated Raman Scattering on the Four-Wave Mixing Process in Birefringent Fibers”, *IEEE/OSA Journal of Lightwave Technology*, vol. 27, no. 22, pp. 4979 – 4988, Nov. 15 2009.

[18] Nuno A. Silva, Nelson J. Muga, and Armando N. Pinto, “Effective Nonlinear Parameter Measurement Using FWM in Optical Fibers in a Low Power Regime”, *To be published on IEEE Journal of Quantum Electronics*, 2009.

[19] G. Agrawal, “Nonlinear Fiber Optics, 4th ed.”, *Academic Press*, 2007.

[20] idQuantique, *id 200 Single-Photon Detector Module - Operating Guide, Version 2.2*, 2005.

[21] D. Goldstein, “Polarized Light, Second Edition, Revised and Expanded”, *CRC Press*, 2003.

[22] N. Gisin, J.-P. von der Weid, and J.-P. Pellaux, “Polarization mode dispersion of short and long single-mode fibers”, *Journal of Lightwave Technology*, vol. 9, pp. 821–827, 1991.

[23] J. P. Gordon and H. Kogelnik, “PMD fundamentals: Polarization mode dispersion in optical fibers”, *Proceedings of the National Academy of Science*, vol. 97, pp. 4541–4550, Apr. 2000.

[24] M. F. Ferreira, A. N. Pinto, P. S. André, N. J. Muga, J. E. Machado, R. N. Nogueira, S. V. Latas, M. H. Sousa, and J. F. Rocha, “Polarization Mode Dispersion in High-Speed Optical Communication Systems”, *Fiber and Integrated Optics*, vol. 24, pp. 261–285, 2005.

[25] G. B. Xavier, G. Vilela de Faria, G. P. Temporão, and J. P. von der Weid, “Full polarization control for fiber optical quantum communication systems using polarization encoding”, *Optics Express*, vol. 16, pp. 1867–1873, 2008.

[26] G. B. Xavier, N. Walenta, G. Vilela de Faria, G. P. Temporão, N. Gisin, H. Zbinden, and J. P. von der Weid, “Experimental polarization encoded quantum key distribution over optical fibres with real-time continuous birefringence compensation”, *New Journal of Physics*, vol. 11, no. 4, pp. 045015, Apr. 2009.

[27] S. Dürr, T. Nonn, and G. Rempe, “Fringe visibility and which-way information in an atom interferometer”, *Phys. Rev. Lett.*, vol. 81, no. 26, pp. 5705–5709, Dec 1998.